Trench Wave Generation by Incident Baroclinic Rossby Waves

JUDITH Y. HOLYER

School of Mathematics, University of Bristol, Bristol BS8 1TP, England

LAWRENCE A. MYSAK†

Departments of Mathematics and Oceanography, University of British Columbia, Vancouver, B.C. V6T 1Y4 Canada

(Manuscript received 28 September 1984, in final form 4 February 1985)

ABSTRACT

We consider the response of a two-layer fluid in a coastal trench to the incidence of low-frequency Rossby waves from the open ocean. While both barotropic and baroclinic incident waves have been incorporated into the theory, the focus of this paper is on the nature of the response in the trench to first-mode baroclinic Rossby waves. In particular, we show that in both the Izu and Peru trenches, deep (lower-layer) longshore currents of O(5 cm s^{-1}) are generated by annual-period Rossby waves whose interfacial amplitude is 5 m. The longshore current speed is particularly large (up to 8 cm s^{-1}) when the longshore wavenumber (l) and frequency (ω) of the incident wave are close to the complex (ω, l) roots of the free trench-wave dispersion relation for a β-plane.

In view of the published evidence (summarized by Magaard) of annual-period Rossby waves in the vicinity of the Izu trench, it is conjectured that forced trench waves of the type described here may be detected in this trench from measurements of subthermocline currents.

1. Introduction

Recently two mechanisms have been proposed for the generation of trench waves: (i) transverse oscillations in a western boundary current flowing across the trench and (ii) a traveling wind system that moves parallel to the trench (Mysak and Willmott, 1981). However, since the basic model used by Mysak and Willmott is barotropic, the results appear to have limited applicability to the strongly stratified trenches of the Pacific Ocean. Indeed, Brink (1983) showed that when continuous stratification is incorporated into the theory for wind-generated long trench waves, the results regarding mechanism (ii) of Mysak and Willmott change considerably. Since in a stratified ocean the trench waves are bottom-trapped, Brink found that the coupling between the wind-driven surface currents and those associated with the trench waves is very weak. (This result is also consistent with the findings of Suarez (1971) who showed that the wind is not an efficient generating mechanism for bottom-intensifed topographic Rossby waves in the open ocean.)

The main purpose of this paper is to describe a third mechanism for trench wave generation: incident baroclinic Rossy waves. In the theory presented here, the stratification is modeled by a two-layer fluid, and in both the trench and offshore region, the β-plane is employed. The important effects of a variable Coriolis parameter on the propagation of free barotropic trench waves have been recently described by Willmott and Bird (1983). From the results of numerical calculations for the Izu and Peru trenches, we conclude that this generation mechanism may be the most efficient of the three proposed.

The results obtained in this paper may also shed some light on the fate of annual-period Rossby waves in the central North Pacific. In the latitude band 30–40°N, Kang and Magaard (1980) and others have observed the presence of free first-mode baroclinic annual Rossby waves which travel in a generally westward direction (with respect to both phase and group velocities). Such waves are generated in the eastern Pacific by the strong annual signal in the wind stress off California (White and Saur, 1981) and by north–south oscillations of annual period in the eastern boundary current off the British Columbia-Washington coast (Mysak, 1983). However, to date there have been no theoretical or observational studies of the behavior of these surface-intensified waves in the western North Pacific. It is shown in this paper that in the southwestern Pacific (at around 30°N), the westward-traveling Rossby waves are reflected by the Izu trench (the southern extension of the Japan trench). However, because of the mismatch of the vertical structure between baroclinic Rossby waves and free trench waves at the outer edge of the trench,

† Also member, Institute of Applied Mathematics, University of British Columbia.

northward-traveling trench waves are generated in the reflection process. It is suggested that the deep longshore currents associated with the forced trench waves should be detectable by an array of moored current meters in the Izu trench.

The outline of this paper is as follows. In Section 2 the coupled vorticity equations for the trench and Rossby waves are derived. In Section 3 these equations are solved for the mass transport streamfunction which describes the trench wave motion that is excited by an incident Rossby wave field. In Section 4 the results are applied to the Izu and Peru trenches for the case of annual and semiannual incident baroclinic Rossby waves. The conclusions are given in Section 5.

2. Governing equations

We consider the motion of a two-layer fluid on a midlatitude β-plane bounded on one side by a coastal trench (Fig. 1a). To allow for arbitrary trench orientation, the x, y coordinates are rotated clockwise from the usual east, north directions through an angle ν (see Fig. 1b). Note that in our model, the continental shelf has been replaced by a vertical wall at $x = 0$. This approximation filters out the relatively high-frequency (periods of days) shelf waves from the problem. In practice, such waves would not be generated by incident baroclinic Rossby waves because of the mismatch in frequency scales: the latter waves have typical periods of several months to years. Also, we remark that Mysak and Magaard (1983) used this vertical-wall approximation in their study of baroclinic Rossby waves incident on the Hawaiian Ridge. The Coriolis parameter for our rotated coordinate system is given by (Willmott and Bird, 1983)

$$f = f_0 + \beta_c y - \beta_s x \tag{2.1}$$

where $\beta_c = \beta \cos\nu$, $\beta_s = \beta \sin\nu$, $f_0 = 2\Omega \sin\theta_0$ and $\beta = 2\Omega \cos\theta_0/R$ with θ_0 the reference latitude of the β-plane, Ω the earth's angular velocity and R the earth's radius.

The linearized equations for two-layer, nondivergent motions on a β-plane with a nonuniform lower layer depth $H_2(x)$ are

$$u_{1t} - fv_1 + \rho_1^{-1} p_{1x} = 0, \tag{2.2a}$$

$$v_{1t} + fu_1 + \rho_1^{-1} p_{1y} = 0, \tag{2.2b}$$

$$(u_{1x} + v_{1y})H_1 - \eta_t = 0, \tag{2.3}$$

and

$$u_{2t} - fv_2 + \rho_2^{-1} p_{1x} + g'\eta_x = 0, \tag{2.4a}$$

$$v_{2t} + fu_2 + \rho_2^{-1} p_{1y} + g'\eta_y = 0, \tag{2.4b}$$

$$(u_2 H_2)_x + v_{2y} H_2 + \eta_t = 0, \tag{2.5}$$

where u_1, v_1 and u_2, v_2 are the velocity components in the x, y directions in the upper and lower layers respectively, p_1 is the pressure just below the surface (assumed rigid), η is the displacement of the interface from its equilibrium level at $z = -H_1$ and $g' = g(\rho_2 - \rho_1)/\rho_2$ is the reduced gravity. We make the Boussinesq approximation and assume that the difference between ρ_1 and ρ_2 is only important in the buoyancy terms involving g'.

Adding the two mass-conservation equations, (2.3) and (2.5), gives

$$(u_1 H_1 + u_2 H_2)_x + (v_1 H_1 + v_2 H_2)_y = 0. \tag{2.6}$$

Hence we define the streamfunction ψ for the vertically averaged velocity by

$$\psi_x = v_1 H_1 + v_2 H_2 \tag{2.7a}$$

$$\psi_y = -(u_1 H_1 + u_2 H_2). \tag{2.7b}$$

Following LeBlond and Mysak (1978, p. 139), we will obtain two coupled equations for ψ and h, where

$$h = \eta - p_1/\rho_1 g. \tag{2.8}$$

For the terms in (2.4) to be of the same order, $\eta \approx p_1/\rho_2 g'$ and so, since $g \gg g'$, $\eta \gg p_1/\rho_1 g$. Thus

$$h \approx \eta. \tag{2.9}$$

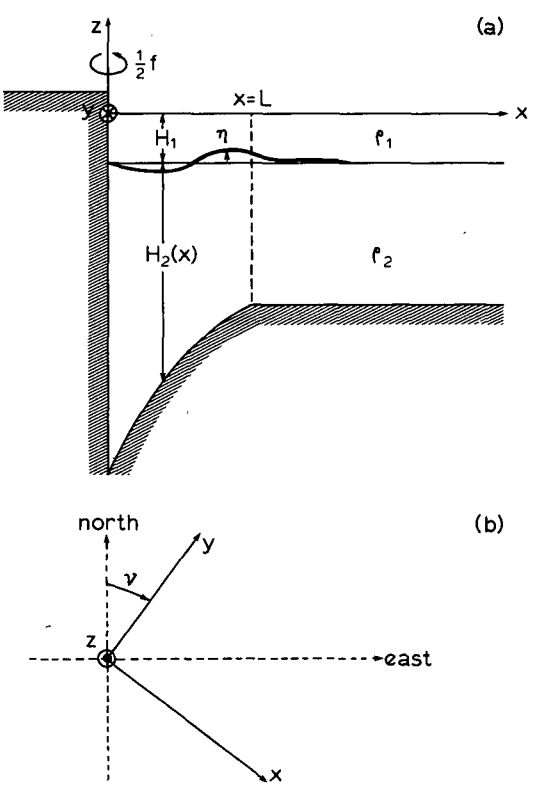

FIG. 1. (a) Cross-section of trench geometry, with longshore coordinate y pointing into the plane. Quantities in the upper and lower layers have a subscript 1 and 2 respectively. Total depth $H = H_1 + H_2$. Over the trench region ($0 \leq x \leq L$) the slope parameter $s = -H_2'/H_2$ is a positive constant. (b) Orientation of x, y coordinates relative to east and north.

Letting $L = \partial^2/\partial t^2 + f^2$, (2.2) and (2.4) give

$$Lu_1 = -\rho_1^{-1}(p_{1xt} + fp_{1y}), \tag{2.10a}$$

$$Lv_1 = -\rho_1^{-1}(p_{1yt} - fp_{1x}), \tag{2.10b}$$

$$Lu_2 = -[g'\eta_{xt} + \rho_2^{-1}p_{1xt} + f(\rho_2^{-1}p_{1y} + g'\eta_y)], \tag{2.11a}$$

$$Lv_2 = -[g'\eta_{yt} + \rho_2^{-1}p_{1yt} - f(\rho_2^{-1}p_{1x} + g'\eta_x)]. \tag{2.11b}$$

Subtracting (2.10a) from (2.11a) gives

$$Lu_2 - Lu_1 = -g'(h_{xt} + fh_y), \tag{2.12a}$$

and, from (2.7b) operated on by L,

$$H_2Lu_2 + H_1Lu_1 = -L\psi_y. \tag{2.12b}$$

Solving (2.12) for Lu_1 and Lu_2 gives

$$Lu_1 = [-L\psi_y + g'H_2(h_{xt} + fh_y)]/H, \tag{2.13a}$$

$$Lu_2 = [-L\psi_y - g'H_1(h_{xt} + fh_y)]/H, \tag{2.13b}$$

where $H = H_1 + H_2$. Similarly we obtain

$$Lv_1 = [L\psi_x + g'H_2(h_{yt} - fh_x)]/H, \tag{2.14a}$$

$$Lv_2 = [L\psi_x - g'H_1(h_{yt} - fh_x)]/H. \tag{2.14b}$$

We now use the vorticity equations in the two layers to eliminate u_i and v_i. In the upper layer

$$(u_{1y} - v_{1x})_t - \beta_c v_1 + \beta_s u_1 - f\eta_t/H_1 = 0, \tag{2.15a}$$

and in the lower layer

$$(u_{2y} - v_{2x})_t - \beta_c v_2 + (\beta_s + fH_2'/H_2)u_2 + f\eta_t/H_2 = 0. \tag{2.15b}$$

Multiplying (2.15a) by H_1 and (2.15b) by H_2 and adding gives, using (2.13) and (2.14),

$$\nabla_h^2\psi_t + \beta_c\psi_x + \beta_s\psi_y + H_2'(f\psi_y - \psi_{xt} + g'H_1h_y)/H_2 = 0, \tag{2.16}$$

where $\nabla_h^2 = \partial^2/\partial x^2 + \partial^2/\partial y^2$, the horizontal Laplacian. Subtracting (2.15a) from (2.15b), operating with L and taking care because L and $\partial/\partial y$ do not commute, gives finally,

$$L(\nabla_h^2h_t + \beta_ch_x + \beta_sh_y) - 2\beta_c(h_{xtt} + fh_{yt}) - 2\beta_s(h_{ytt} - fh_{xt}) - L^2h_t/r^2f^2 + H_2'L \times [L\psi_y + g'H_1(h_{xt} + fh_y)]/g'H_2^2 = 0, \tag{2.17}$$

where $r = \{g'H_1H_2/[f^2(H_1 + H_2)]\}^{1/2}$ is the internal Rossby radius of deformation. Equation (2.16) and (2.17) are the required coupled equations for ψ and h. If $\beta = 0$ the equations reduce to the two-layer variable depth equations given by Mysak (1984). On setting $g' = 0$ in the barotropic equation, (2.16) reduces to the single-layer β-plane equation of Willmott and Bird (1983).

We look for solutions to (2.16) and (2.17) with time-dependence $\exp(-i\omega t)$, with $\omega > 0$. Since we are interested in low-frequency waves (periods of order one year) we assume

$$\omega \ll |f|. \tag{2.18}$$

This approximation will filter out internal Kelvin waves and internal gravity waves. In conjunction with (2.18) we assume

$$\omega\frac{\partial}{\partial x} \ll f\frac{\partial}{\partial y}, \tag{2.19}$$

i.e., that length-scales in x are comparable to length-scales in y. We also assume that

$$H_1 \ll H_2, \tag{2.20}$$

i.e., that the upper layer is thin compared to the lower layer. Hence $H \approx H_2$ and $r^2 \approx g'H_1/f^2$. Finally, we remark that in topographic wave theory, we have that $H_2'f\psi_y/H_2$ [the dominant bottom slope term in (2.16)] is of the order of $\nabla_h^2\psi_t$.

Using the above approximations and the scaling $\psi/h = O(r^2f)$, which implies that baroclinic waves force the topographic waves (and not vice versa), (2.16) and (2.17) simplify to[1]

$$\nabla_h^2\psi + \frac{i\beta_c}{\omega}\psi_x + \frac{i\beta_s}{\omega}\psi_y + \frac{iH_2'f}{\omega H_2}[\psi_y + r^2fh_y] = 0, \tag{2.21}$$

$$\nabla_h^2h + \frac{i\beta_c}{\omega}h_x + \frac{i\beta_s}{\omega}h_y - \frac{h}{r^2} = 0. \tag{2.22}$$

There is a possible alternative scaling for ψ/h, which determines the nature of the coupling between (2.16) and (2.17), namely, $\psi/h = O(H_2r^2f/H_1)$. This was the scaling used by Gratton (1983); it is the appropriate scaling for wind-driven motions in lakes and straits. Gratton's scaling leads to surface-intensified motions in which the topographic waves force the baroclinic (interfacial) field. The scaling $\psi/h = O(r^2f)$ leads to bottom-intensified motions in the trench, which is the expected effect of stratification on trench waves (Brink, 1983); further, it is the only scaling consistent with our approximations. The bottom slope H_2' only appears in the barotropic equation (2.21), which, we note, is forced by the free solution of the baroclinic equation (2.22). Equation (2.22) is the standard baroclinic Rossby wave equation; hence we see that to the order of our approximations, baroclinic Rossby waves are not affected by the bottom topography in this model. We will solve (2.21) and (2.22) by looking for plane-wave solutions in x and y. This is appropriate

[1] A rigorous derivation of (2.21) and (2.22) based on dimensionless variables can easily be done along the lines given in Mysak (1984, p. 92). The key features which allow us to neglect the coupling term involving H_2' in (2.17) are that $\psi = O(r^2fh)$ and the assumptions (2.20) and $\nabla_h^2\psi_t = O(H_2'f\psi_y/H_2)$ (see end of last paragraph).

if we consider bottom profiles with H_2'/H_2 = constant and if we replace f by f_0 in (2.21) and consider r independent of x. The constant f approximation is justifiable provided that the waves under consideration do not travel as far as f_0/β north or south of our reference latitude. For the cases we consider this distance is several thousand kilometers.

3. Reflection and trench wave generation

We suppose that a Rossby wave is incident on the trench shown in Fig. 1. We first determine the solution for the waves generated over the trench and the reflected wave. Then the longshore velocity in the trench will be found. The bottom profile is taken to have the form

$$H_2(x) = \begin{cases} H_0 e^{-sx} & \text{for} \quad x \leqslant L \\ H_0 e^{-sL} & \text{for} \quad x \geqslant L. \end{cases} \tag{3.1}$$

At $x = 0$ we require no flow normal to the wall, which implies, from (2.13),

$$\psi = 0, \quad h = 0 \quad \text{at} \quad x = 0 \tag{3.2}$$

to $O(\omega/f)$. At $x = L$, the bottom slope is discontinuous and continuity of velocity, pressure and interfacial displacement has to be imposed. This results in the jump conditions

$$[h] = 0, \quad [h_x] = 0 \tag{3.3a}$$

$$[\psi] = 0, \quad [\psi_x] = 0 \tag{3.3b}$$

at $x = L$. At infinity we specify the incoming wave energy, and require that the reflected wave has an outgoing group velocity.

We look for plane-wave solutions proportional to $\exp(ily - i\omega t)$. In the deep-sea region $x \geqslant L$, the slope is zero and (2.21) and (2.22) give

$$h = C_I \exp[ik_I(x - L)] + C_R \exp[ik_R(x - L)], \tag{3.4a}$$

$$\psi = T_I \exp[ip_I(x - L)] + T_R \exp[ip_R(x - L)], \tag{3.4b}$$

with

$$\left.\begin{matrix} k_I \\ k_R \end{matrix}\right\} = -\frac{\beta_c}{2\omega} \pm \left[\frac{\beta^2}{4\omega^2} - \frac{1}{r^2} - \left(l + \frac{\beta_s}{2\omega}\right)^2\right]^{1/2}, \tag{3.5a}$$

$$\left.\begin{matrix} p_I \\ p_R \end{matrix}\right\} = -\frac{\beta_c}{2\omega} \pm \left[\frac{\beta^2}{4\omega^2} - \left(l + \frac{\beta_s}{2\omega}\right)^2\right]^{1/2}. \tag{3.5b}$$

In (3.5a, b), $\beta = (\beta_c^2 + \beta_s^2)^{1/2}$, which follows from (2.1). Equations (3.5a, b) give the dispersion relations for baroclinic and barotropic Rossby waves. The positive signs give waves whose energy is incident on the trench (e.g., from the east in Fig. 1), and the negative signs give reflected waves. This follows from the classical slowness curves used for Rossby waves and the fact that energy travels in the direction of the group velocity (LeBlond and Mysak, 1978). Thus the first term in (3.4a) represents an incident baroclinic wave, which will have a known amplitude C_I. The second term is the reflected baroclinic wave, whose amplitude is to be determined. The first term in (3.4b) allows for the possibility of an incident barotropic wave with known amplitude T_I. In this paper we only do numerical examples for the case $T_I = 0$, but we retain the T_I term in the analysis because the same equations could be used to solve the problem of barotropic Rossby waves incident on a trench. It can be seen from (3.11) and (3.12) below that if $T_I = O(r^2 f C_I)$, then the trench wave amplitude generated by an incident barotropic Rossby wave will be of the same order as that generated by an incident baroclinic Rossby wave. However, at annual or semiannual periods (which are used in the numerical examples below), there are no observed barotropic Rossby wave signals in the North Pacific. The second term in (3.4b) is the reflected barotropic wave, which is required to perform the matching at $x = L$, *whether or not* $T_I = 0$. Thus in summary, C_I and T_I are regarded as known and C_R and T_R are to be found by matching at $x = L$.

Over the trench ($0 \leqslant x \leqslant L$) the plane-wave solutions of (2.21) and (2.22) are given by

$$h = C_A e^{ik_I x} + C_B e^{ik_R x}, \tag{3.6a}$$

$$\psi = -r^2 f \frac{C_A e^{ik_I x} + C_B e^{ik_R x}}{1 + \omega/(r^2 fls)} + \exp(-i\beta_c x/2\omega)(T_A e^{i\gamma x} + T_B e^{-i\gamma x}), \tag{3.6b}$$

where

$$\gamma = \left[\frac{\beta^2}{4\omega^2} + \frac{sfl}{\omega} - \left(l + \frac{\beta_s}{2\omega}\right)^2\right]^{1/2}. \tag{3.7}$$

For trench waves, where s is positive, γ is real. The term proportional to $r^2 f$ in (3.6b) is the particular solution of (2.21) forced by the baroclinic solution (3.6a), whereas the remaining part of ψ represents the trench wave solution, whose amplitude will be determined by the incident waves outside the trench. We shall call this part ψ_T. Another form of ψ_T is given in (3.13) below.

The boundary conditions (3.2) at $x = 0$ imply

$$C_B = -C_A, \quad T_B = -T_A. \tag{3.8}$$

Then matching at $x = L$ by using (3.3) determines the remaining coefficients C_A, C_R, T_A, and T_R in terms of the known coefficients C_I and T_I. From (3.3a) we find

$$C_A = C_I \exp(-ik_I L), \tag{3.9}$$

$$C_R = -C_I \exp[i(k_R - k_I)L]. \tag{3.10}$$

From (3.3b) we obtain

$$2T_A\left[i\left(p_R+\frac{\beta_c}{2\omega}\right)\sin\gamma L-\gamma\cos\gamma L\right]$$
$$=\left\{\frac{r^2fC_I}{(1+\omega/r^2fls)}\left[p_R-k_I-(p_R-k_R)\exp(i(k_R-k_I)L)\right]+T_I(p_R-p_I)\right\}\exp(i\beta_cL/2\omega), \quad (3.11)$$

$$T_R\left[i\left(p_R+\frac{\beta_c}{2\omega}\right)\sin\gamma L-\gamma\cos\gamma L\right]=\frac{-r^2fC_I}{(1+\omega/r^2fls)}\left\{i\left(k_I+\frac{\beta_c}{2\omega}\right)\sin\gamma L-\gamma\cos\gamma L-\exp[i(k_R-k_I)L]\left[i\left(k_R+\frac{\beta_c}{2\omega}\right)\sin\gamma L-\gamma\cos\gamma L\right]\right\}-T_I\left[i\left(p_I+\frac{\beta_c}{2\omega}\right)\sin\gamma L-\gamma\cos\gamma L\right]. \quad (3.12)$$

The (forced) trench wave part of the stream function solution (3.6b) is given by

$$\psi_T=2T_Ai\exp(-i\beta_cx/2\omega)\sin\gamma x, \quad (3.13)$$

where (3.8) has been used and T_A is given by (3.11).

If there are no incident waves ($T_I=C_I=0$), we obtain the dispersion relation for free trench waves on a two-layer β-plane. By (3.11) it is

$$\left[i\left(p_R+\frac{\beta_c}{2\omega}\right)\sin\gamma L-\gamma\cos\gamma L\right]=0. \quad (3.14)$$

This dispersion relation is the same as that obtained by Willmott and Bird (1983) for waves on a single layer β-plane if we set the shelf width to zero in their model and make the low-frequency approximation. The presence of the two layers does not affect the dispersion relation. There are no solutions to (3.14) with l and ω real. This implies that there are no unattenuated "leaky" modes which consist of incoming and outgoing waves; such "leaky" propagating waves, however, can exist in edge wave theory (e.g., see LeBlond and Mysak, 1978). The "leaky" trench waves plotted by Willmott and Bird (1983) are not true leaky modes in the above sense since they contain only outgoing wave energy. Further, since the (ω, l) pairs chosen by Willmott and Bird for plotting purposes do not satisfy the dispersion relation, the jump conditions analogous to (3.3) are not satisfied.

If there were real solutions to (3.14) we would get, for suitable parameters of the incident wave, a true resonance with infinite amplitudes for the (forced) trench wave. There will, however, be large values for the trench wave amplitude when the values for l and ω are close to complex solutions of (3.14), the so-called normal modes.

In the Appendix we obtain the energy equation for the model and show that to within the approximations made here, the incident energy equals the reflected energy.

Since topographic waves trapped along a coast generally have larger longshore velocities than offshore velocities, it is useful to analyze the expressions for v_i as given by (2.14). Invoking the approximations (2.18)–(2.20) in (2.14), we obtain

$$v_1=(\psi_x-r^2fH_2h_x/H_1)/H, \quad (3.15a)$$

$$v_2=(\psi_x+r^2fh_x)/H. \quad (3.15b)$$

Since $\psi/h=O(r^2f)$ and $H_2\gg H_1$, (3.15a) implies that v_1 is dominated by the longshore velocity associated with the incident baroclinic Rossby wave, viz., $-r^2fh_x/H_1$ [to $O(H_1/H_2)$], unless the trench wave has a resonant response $O(H_2/H_1)$ larger than the typical response. In (3.15b) we substitute for ψ the expression given by (3.6b), in which (3.6a) has been used in the first term and the definition of ψ_T has been used; this yields

$$v_2=\frac{1}{H}\left[\psi_{Tx}+\frac{\omega h_x}{ls}\left(1+\frac{\omega}{r^2fls}\right)^{-1}\right]. \quad (3.16)$$
$$\qquad\qquad (1)\qquad\qquad (2)$$

Since (2)/(1) = $O(\omega/r^2fls)$ in (3.16), it follows that if

$$\omega/r^2fls\ll 1, \quad (3.17)$$

the longshore current in the lower layer is dominated by the trench wave contribution, viz., ψ_{Tx}/H. For annual-period, midlatitude waves with wavelengths on the order of several hundred kilometers, we find $\omega/(r^2fls)=O(10^{-2})$ using $s=O(10^{-5}\ m^{-1})$ (which characterizes most Pacific trenches—see Mysak *et al.*, 1979). Only if $\omega/f\gtrsim 10^{-1}$, does the inequality (3.17) break down. Thus we conclude that low-frequency baroclinic Rossby waves incident in a midlatitude trench will generate deep longshore currents that are almost exclusively associated with the trench waves. This analysis also indicates that in order to detect Rossby wave generated trench waves with current meters, one should make measurements below the thermocline, since above it the (longshore) currents will be mainly due to the Rossby waves. Combining $\partial/\partial x$ of (3.13) with $e^{ily-i\omega t}$, letting $T_A=|T_A|e^{i\theta}$ and then taking the real part, we arrive at the following expression for the trench wave longshore velocity in the lower layer:

$$v_{2T} \equiv \frac{\Psi_{Tx}}{H} = \frac{|T_A|}{H}\left\{\left(\frac{\beta_c}{2\omega}+\gamma\right)\sin\left(\gamma x+\frac{\beta_c}{2\omega}x - ly+\omega t-\theta\right)+\left(\frac{\beta_c}{2\omega}-\gamma\right)\times\sin\left[\gamma x-\left(\frac{\beta_c}{2\omega}x-ly+\omega t-\theta\right)\right]\right\}. \quad (3.18)$$

A good estimate for the maximum longshore lower-layer velocity in the trench is given by $2|T_a|\ \max(\gamma, \beta_c/2\omega)/H$. This is the maximum modulus of (3.18) when it is written in its complex exponential form and it occurs at $x = 0, \pi/\gamma, 2\pi/\gamma, \ldots$. The maximum value of v_{2T} as given by (3.18), on the other hand, will vary with x, y and t. Generally, $\beta_c/2\omega < \gamma$; hence we shall use $2|T_A|\gamma/H$ as a measure of the (lower-layer) longshore current speed associated with a trench wave (see Section 4). The maximum longshore velocity will in fact always be less than or equal to this measure. However, there will always be a value of y, for fixed t, and a value of t for fixed y, for which $2|T_A|\gamma/H$ is the true maximum speed.

4. Forced trench waves in the Izu and Peru trenches

a. *The Izu trench*

The southern extension of the Japan trench, the Izu trench, is one possible region where trench waves may be generated by incident Rossby waves. The Izu trench is oriented north–south and is centered at 30°N; hence it is fairly far removed from the intense eastward-flowing Kuroshio, more than 5° to the north. At around 30°N and to the east of the Izu trench, annual-period ($\omega = 2 \times 10^{-7}$ s^{-1}), first-mode, westward-traveling baroclinic Rossby waves have been detected by an analysis of subsurface temperature records (e.g., see Kang and Magaard, 1980; Magaard, 1983). In view of these observations, it is of considerable interest to estimate the lower-layer longshore trench wave current excited by these incident waves.

The values of the model parameters which characterize the Izu trench region are given by

$$\left.\begin{aligned} &f = 0.73 \times 10^{-4}\ \text{s}^{-1}\\ &\beta = 2.0 \times 10^{-11}\ \text{m}^{-1}\ \text{s}^{-1}\end{aligned}\right\}\ \text{at } 30°\text{N}$$
$$r = 45\ \text{km},\quad \text{Emery } \textit{et al.}, (1984)$$
$$\nu = 0°$$
$$H = 5\ \text{km},\quad \text{ambient ocean depth}$$
$$s = 6.5 \times 10^{-6}\ \text{m}^{-1}\ (= -H_2'/H_2)$$
$$L = 45\ \text{km},\quad \text{trench width} \quad (4.1)$$

Hence we find that at the annual period, $\omega/(fr^2ls) = O(10^{-2})$ for $l = O(10^{-5}\ \text{m}^{-1})$ (typical Rossby wave longshore wave number). Thus according to our criterion (3.17), the lower-layer longshore current in the trench excited by the incident Rossby waves will be that associated with a trench wave.

Figure 2 shows our upper-bound estimate of the lower-layer longshore current ($2|T_A|\gamma/H$—see Section 3) as a function of the longshore wave number l (of both the incident Rossby wave and the forced trench wave) and the incidence angle α [obtained from (A6)]. From the slowness circle in Fig. 2, we note that if $0 < \alpha < \pi/2$, then $l > 0$ also. Thus in this range of α the incident wave energy is propagating toward the southwest, and the forced trench-wave phase propagation is northward along the trench, in the same direction as for a free trench wave. (In the northern hemisphere, free trench waves travel with the coast on the left.) The forced trench waves only have large amplitudes when they are excited by incident Rossby waves for which $0 < \alpha < \pi/2$. Southward-traveling forced waves will be excited by incident Rossby waves for which $-\pi/2 < \alpha < 0$ (i.e., $l < 0$), but their amplitudes are very small since they travel opposite to the direction of free trench waves.

From Fig. 2 we note that an incident wave of interfacial amplitude 5 m, which is characteristic of this region (Kang and Magaard, 1980), produces an ambient trench current of about 1.5 cm s^{-1}. The amplitudes at the "resonant" peaks (labeled A, B, C, D) are, however, several times larger, ranging from about 3 to 7.5 cm s^{-1}. The properties of the incident waves at these peaks are given in Table 1. As remarked in Section 3, such peaks correspond to ω, l pairs which are close to the complex solutions (normal modes) given by the free wave dispersion relation (3.14). If (3.14) had real solutions for (ω, l), these peaks would have infinite amplitudes. On an f-plane long trench waves are nondispersive, and have a real dispersion relation of the form

$$\omega = c_j l \quad (4.2)$$

for each offshore mode j, where c_j is independent of l and $c_1 > c_2 > \cdots$ (Mysak *et al.*, 1979). On a β-plane the normal modes, at long wavelengths, have a dispersion relation whose real part is similar to (4.2). Note that for fixed ω, (4.2) implies that as l decreases, we jump to a larger value of c_j, i.e., to a lower mode. Thus as one moves to the left in Fig. 2 (i.e., to lower wave numbers), successively lower "modes" are generated at the resonant peaks. As a general rule, the number of zero crossings of the wave amplitude in the offshore direction decreases with mode number.

Figure 3 shows the offshore structure of the forced trench-wave longshore current excited by the resonant wave number at B in Fig. 2 at $y = 0$, $t = 0$, found from (3.18). At other values of y and t, the structure will be similar. For this value of l, $\omega/fr^2ls = 0.86 \times 10^{-2}$, in accordance with (3.17) and our remarks made earlier in this section. Note that the largest current amplitude (6.8 cm s^{-1}) occurs at $x = 39$ km, near the outer edge of the trench, and that this value

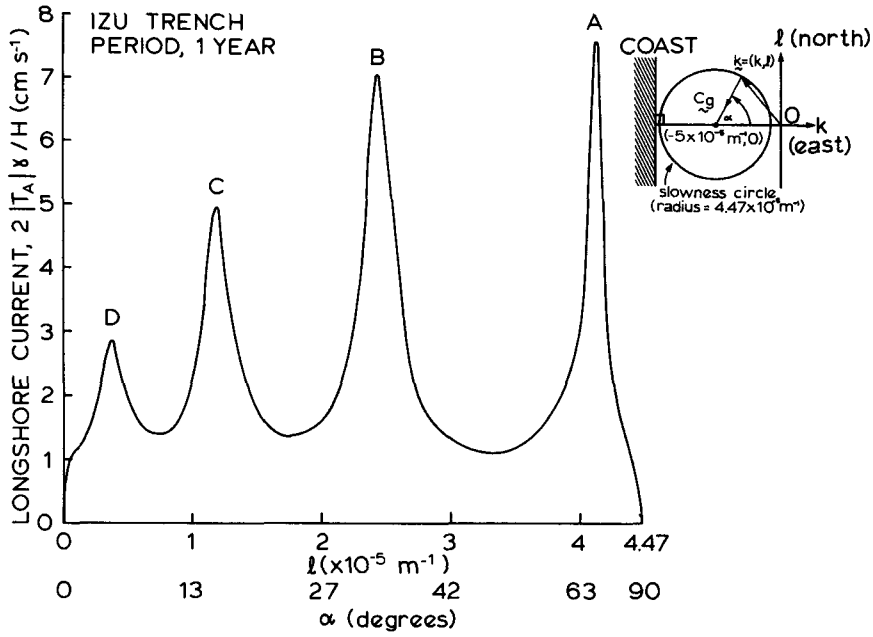

FIG. 2. Estimate of lower-layer longshore current in Izu trench generated by an annual-period Rossby wave of amplitude C_I = 5 m. Since the current depends linearly on C_I, the response for other incident wave amplitudes can readily be obtained from this figure. The longshore wavenumber is l and α is the incidence angle (the angle between the incident group velocity $\mathbf{c}_g$ and the normal to the coast—see inset). The incident wave properties at the "resonant" peaks (labelled A, B, C and D) are given in Table 1.

is only a few percent less than the Fig. 2 upper-bound estimate of 7.1 cm s^{-1} for this value of l. Thus it appears that the estimated current magnitude given in Fig. 2 is a good indication of the actual maximum current speed, at least for this example. Finally, we observe that the excited wave is most closely related to the third mode since ψ_T for such a mode will have three zero crossings in $0 < x < L$, and when differentiated with respect to x, would yield four zero crossings for v_{2T}, as shown in Fig. 3.

For a 6-month period baroclinic Rossby wave the slowness circle is considerably smaller (radius = 1.12×10^{-5} m^{-1}) than that for the annual wave (radius = 4.47×10^{-5} m^{-1}). Thus the range of longshore wave numbers which can generate a trench wave is reduced to $0 < l < 1.12 \times 10^{-5}$ m^{-1}, which characterizes relatively long Rossby waves (wavelengths > 400 km). Accordingly, the number of resonant peaks (and hence the number of modes) is reduced to two in this case (Fig. 4). Also, for the same amplitude incident wave (C_I = 5 m), the longshore current generated in the trench is much weaker than in the annual case, ranging from about 0.4 to 1.2 cm s^{-1}. Thus the detection of 6-month forced trench

TABLE 1. Properties of the incident annual Rossby wave at each of the "resonant" peaks in Fig. 2 (Izu trench). Also given for each peak is the estimate (upper bound) of the longshore current generated in the lower layer.

Resonant peak	Incidence angle α (degrees)	Longshore wavenumber† l ($\times 10^{-5}$ m^{-1})	Incidence wavelength $2\pi/(k_I^2 + l^2)^{1/2}$ (km)	Generated longshore current (cm s^{-1})
A	67	4.12	119	7.53
B	33	2.44	230	7.06
C	16	1.2	423	4.91
D	4.8	0.375	951	2.86

† For both the incident Rossby wave and the forced trench wave.

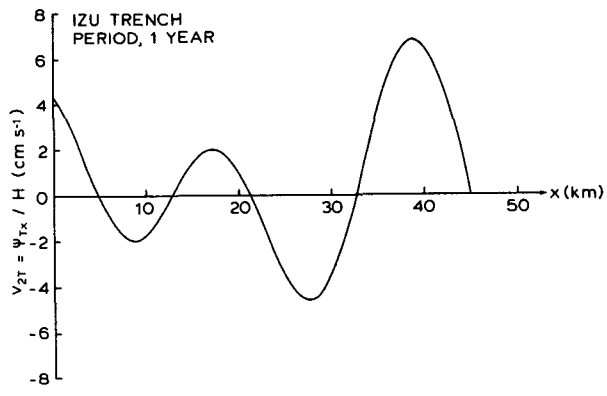

FIG. 3. Lower-layer longshore current of forced annual-period trench wave in Izu trench as a function of offshore distance x. v_{2T} is computed from (3.18) with $y = 0$, $t = 0$, C_I = 5 m and $l = 2.44 \times 10^{-5}$ m^{-1} (corresponding to B in Fig. 2).

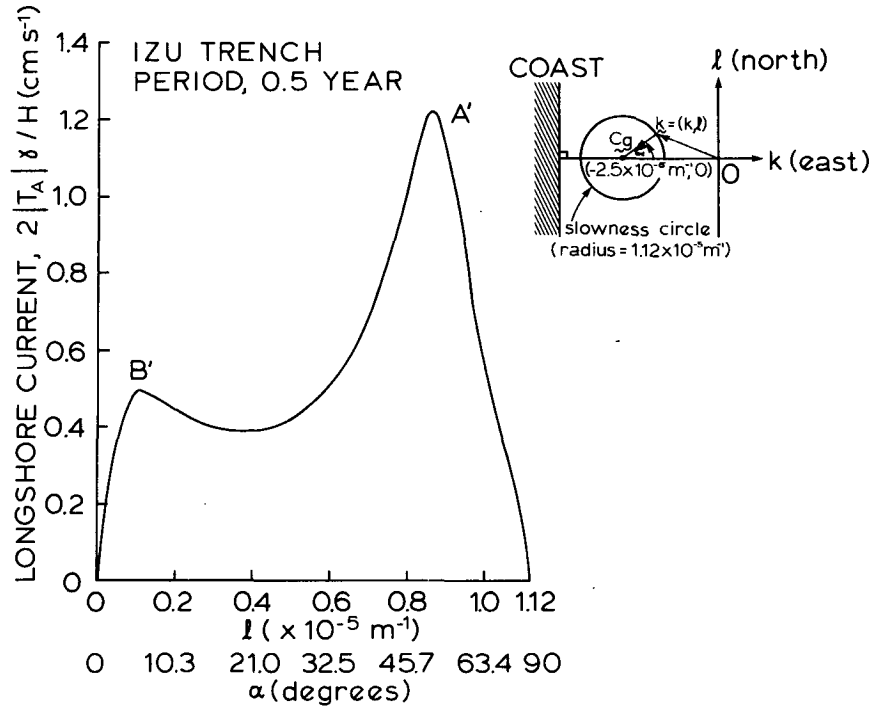

FIG. 4. Estimate of lower-layer longshore current in Izu trench generated by a 6-month period Rossby wave of amplitude C_I = 5 m. l and α are the longshore wavenumber and incidence angle respectively (see inset). The incident wave properties at the "resonant" peaks (labelled A′ and B′) are given in Table 2.

waves is highly unlikely. The offshore structure of the longshore current excited by a Rossby wave resonant at A′ in Fig. 4 is shown in Fig. 5. With two zero crossings, v_{2T} in Fig. 5 would be associated with a first-mode wave. Note that the maximum amplitude (1.21 cm s^{-1}) occurs at x = 30 km and is also just under the upperbound estimate shown in Fig. 4 (1.22 cm s^{-1}, see also Table 2).

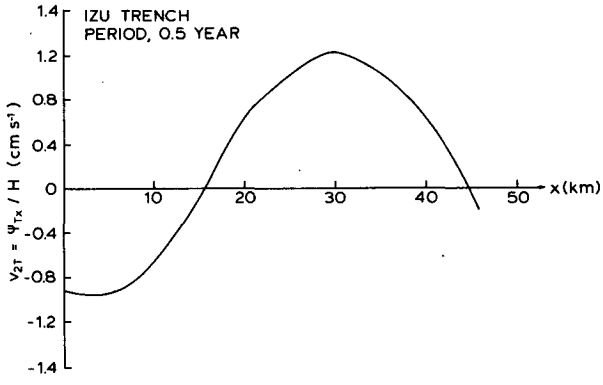

FIG. 5. Lower-layer longshore current of forced 6-month period trench wave in Izu trench as a function of offshore distance x. v_{2T} is computed from (3.18) with y = 0, t = 0, C_I = 5 m and l = 0.87 × 10^{-5} m^{-1} (corresponding to A′ in Fig. 4).

b. The Peru trench

The Peru trench lies in the southeastern part of the South Pacific at a central latitude of about 15°S and with a southeast–northwest orientation. The surface winds in the central tropical Pacific have (among others) a notable annual signal which appears to generate, through a remote forcing mechanism involving the equatorial wave guide, a local warming (the annual El Niño) off Peru every January–March (Busalacchi and O'Brien, 1981). It is conceivable that such winds could also generate low-latitude annual Rossby waves in the central South Pacific whose energy is partly directed toward the east, i.e., incident

TABLE 2. Properties of the incident 6-month Rossby wave at each of the "resonant" peaks in Fig. 4 (Izu trench). Also given for each peak is the estimate of the longshore current generated in the lower layer.

Resonant peak	Incidence angle α (degrees)	Longshore wavenumber† l (×10^{-5} m^{-1})	Incident wavelength $2\pi/(k_I^2 + l^2)^{1/2}$ (km)	Generated longshore current (cm s^{-1})
A′	51	0.87	315	1.22
B′	6.2	0.12	451	0.50

† For both the incident Rossby wave and the forced trench wave.

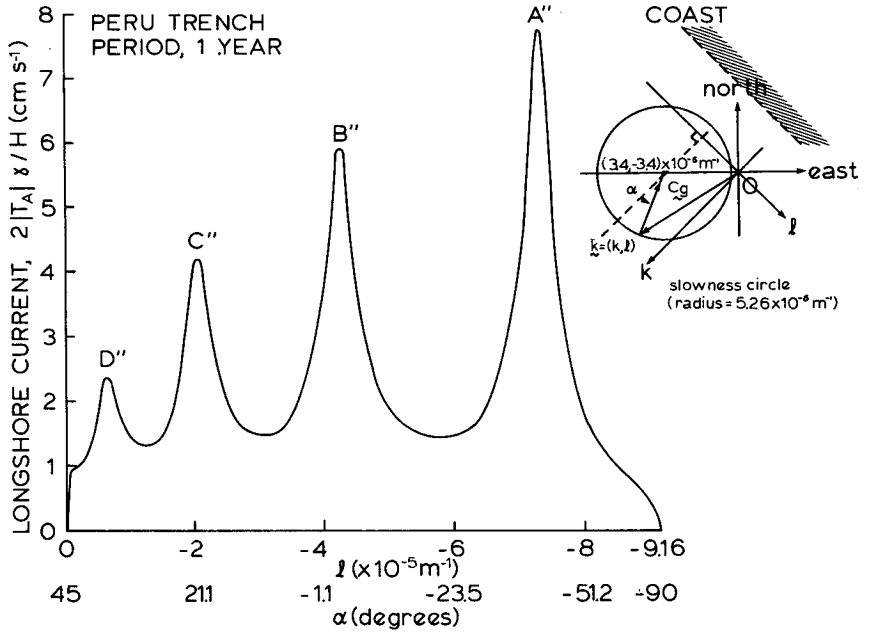

FIG. 6. Estimate of lower-layer current in Peru trench generated by an annual-period Rossby wave of amplitude C_I = 5 m. l and α are the longshore wavenumber and incidence angle respectively (see inset). The incident wave properties at the "resonant" peaks (labelled A", B", C" and D") are given in Table 3.

on the Peru trench. The slowness circle for the annual wave implies that such waves have a much shorter wavelength (<100 km) than those incident on the trenches in the western Pacific (compare insets in Figs. 2 and 6).

The values of the model parameters which characterize the Peru trench region are given by

$$\left.\begin{aligned} &f = -0.376 \times 10^{-4}\ \text{s}^{-1} \\ &\beta = 2.2 \times 10^{-11}\ \text{m}^{-1}\ \text{s}^{-1} \end{aligned}\right\}\ \text{at } 15°\text{S}$$
$$r = 61\ \text{km}, \quad \text{Brink, (1982)}$$
$$\nu = 135°$$
$$H = 5\ \text{km}$$
$$s = 5.68 \times 10^{-6}\ \text{m}^{-1}$$
$$L = 50\ \text{km} \qquad (4.3)$$

Hence we find that at the annual period, $\omega/(fr^2ls) = O(5 \times 10^{-3})$ for $l = O(-5 \times 10^{-5}\ \text{m}^{-1})$ (see Fig. 6). Thus according to (3.17) the lower-layer longshore current in the trench will be associated with that of a forced trench wave travelling toward the equator.

Figure 6 shows our upper-bound estimate for the lower-layer longshore current as a function of the incident longshore wave number. As in the case for the Izu trench only those wavenumbers which have the same sign as those for free trench waves (namely, $l < 0$ in this case) produce currents of substantial amplitude. Figure 6 also shows four resonant peaks with amplitudes comparable to those found in Fig. 2 (see also Tables 1 and 3). As an example of the offshore structure for one of the resonant wavenumbers, Fig. 7 shows $v_{2T}(x)$ evaluated at point A" in Fig. 6. The maximum current speed (at $x \approx 45$ km) is 7.6 cm s^{-1}, which is again very close to the upper-bound estimate (7.75 cm s^{-1}—see Table 3). The five zero crossings in Fig. 7 indicate that a fourth-mode wave has been excited at point A".

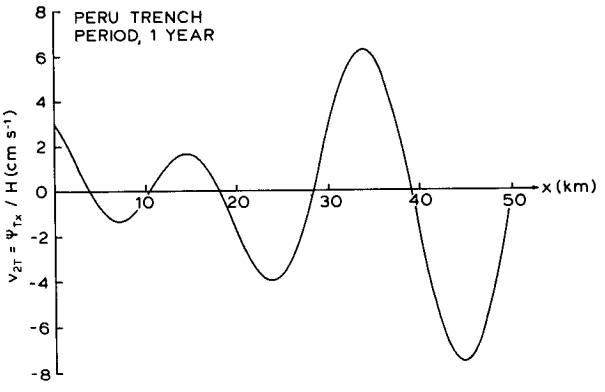

FIG. 7. Lower-layer longshore current of forced annual-period trench wave in Peru trench as a function of offshore distance x. v_{2T} is computed from (3.18) with $y = 0$, $t = 0$, $C_I = 5$ m and $l = -7.31 \times 10^{-5}$ m^{-1} (corresponding to A" in Fig. 6).

TABLE 3. Properties of the incident annual Rossby wave at each of the "resonant" peaks in Fig. 6 (Peru trench). Also given for each peak is the estimates of the longshore current generated in the lower layer.

Resonant peak	Incidence angle α (deg)	Longshore wavenumber† l ($\times 10^{-5}$ m^{-1})	Incident wavelength $2\pi/(k_i^2 + l^2)^{1/2}$ (km)	Generated longshore current (cm s^{-1})
A′	−40	−7.31	58.4	7.75
B′	−3.8	−4.25	62.3	5.88
C′	20	−2.07	69.3	4.19
D′	39	−0.60	78.3	2.33

† For both the incident Rossby wave and the forced trench wave.

5. Conclusions

We have shown that annual-period, first-mode baroclinic Rossby waves can generate deep (lower-layer) longshore currents of O(5 cm s^{-1}) in both the Izu and Peru trenches. The forced trench waves have relatively large amplitudes ("resonances) when the longshore wave number and frequency of the incident wave are close to the complex roots of the free trench-wave dispersion relation for a β-plane. For each trench there are four such resonant responses in the graph depicting the estimated longshore current speed; these peaks range from 3 to 8 cm s^{-1}. For incident waves with longshore wavenumber of opposite sign to that of the free trench waves, the forced longshore currents in the trench are negligible. Also, for incident baroclinic waves of 6-month period, the longshore currents associated with the forced waves appear to be quite small [of O(1 cm s^{-1}) in the Izu trench].

Although the focus in this paper has been on trench wave generation by incident *baroclinic* Rossby waves, the analysis has been carried out in a manner which would enable one to determine explicitly the response due to *barotropic* waves. Also, by changing the sign of H_2' but still allowing the interface to intersect a vertical wall at $x = 0$, (i.e., on-shelf stratification over a deep shelf), the solution obtained here could be used to find the amplitudes of low-frequency shelf waves generated by either baroclinic or barotropic Rossby waves. Since we have used the low-frequency approximation $\omega \ll |f|$, no internal Kelvin waves would be generated along the coast and hence the difficult problem of shelf–Kelvin wave coupling over a two-layer stratified shelf is avoided (e.g., see Allen, 1975).

Since the Rossby waves with a westward component to the group velocity are substantially longer than those with an eastward component and hence are less susceptible to dissipation and nonlinear affects, the Izu trench is a likely region to search for annual-period trench waves that are excited by westward-traveling Rossby waves. Magaard (1983) has shown that to the east of the Izu trench the first vertical mode Rossby wave potential energy density at the one-year period has a relatively large amplitude (see lower left corner of his Fig. 3). We conjecture that this intensification of the wave energy may be an indication of Rossby wave reflection by the Izu trench and hence, by the theory presented in this paper, indirect evidence of forced annual-period trench waves.

Acknowledgments. This work was completed during a visit (Summer 1984) by J.Y.H. to the University of British Columbia. The authors thank Ken Brink for his comments on a first draft of this paper. The support of the U.S. Office of Naval Research, Code PO422, and the Canadian Natural Sciences and Engineering Research Council are gratefully acknowledged.

APPENDIX

The Energetics for the System

Taking the scalar product of (2.2) with $\rho_1 H_1 \mathbf{u}_1$ and adding the scalar product of (2.4) with $\rho_2 H_2 \mathbf{u}_2$ gives,

$$\frac{\partial}{\partial t}\left[\frac{1}{2}\rho_1 H_1(u_1^2 + v_1^2) + \frac{1}{2}\rho_2 H_2(u_2^2 + v_2^2)\right] + p_{1x}(H_1 u_1 + H_2 u_2) + p_{1y}(H_1 v_1 + H_2 v_2) + \rho_2 g' H_2(\eta_x u_2 + \eta_y v_2) = 0. \quad \text{(A1)}$$

Then using (2.3) and (2.5) in (A1) we obtain

$$\frac{\partial}{\partial t}\left[\frac{1}{2}\rho_1 H_1(u_1^2 + v_1^2) + \frac{1}{2}\rho_2 H_2(u_2^2 + v_2^2) + \frac{1}{2}\rho_2 g'\eta^2\right] + \nabla\cdot[p_1(\mathbf{u}_1 H_1 + \mathbf{u}_2 H_2) + \rho_2 g' H_2 \mathbf{u}_2 \eta] = 0. \quad \text{(A2)}$$

This is the energy equation for a two-layer β-plane model with arbitrary H_1, H_2 and ρ_1, ρ_2. The energy per unit area is given by [see (A2)]

$$E = \frac{1}{2}\rho_1 H_1(u_1^2 + v_1^2) + \frac{1}{2}\rho_2 H_2(u_2^2 + v_2^2) + \frac{1}{2}\rho_2 g'\eta^2. \quad \text{(A3)}$$

Outside the trench, where the waves are propagating, the energy comes in as a baroclinic and a barotropic part. Using (2.13) and (2.14) in (A3) it is easy to show that the average energy per unit area is given by

$$\langle E\rangle = \frac{1}{4}\rho g' r^2\left(k^2 + l^2 + \frac{1}{r^2}\right)|h_0|^2 \quad \text{(A4)}$$

for baroclinic Rossby waves, and by

$$\langle E \rangle = \frac{1}{4H} \rho(k^2 + l^2)|\psi_0|^2 \quad \text{(A5)}$$

for barotropic Rossby waves, where h_0 and ψ_0 are the complex amplitudes of the baroclinic and barotropic waves respectively. For baroclinic waves the group velocity is

$$c_g = (\partial\omega/\partial k, \partial\omega/\partial l)$$
$$= -(k^2 + l^2 + r^{-2})^{-1}[\beta_c + 2k\omega, \beta_s + 2l\omega], \quad \text{(A6)}$$

and for barotropic waves,

$$c_g = -(k^2 + l^2)^{-1}[\beta_c + 2k\omega, \beta_s + 2l\omega]. \quad \text{(A7)}$$

Thus the energy flux incident on the trench is, using (3.4) and (A4)–(A7),

$$\frac{1}{4} \rho g' r^2(\beta_c + 2k_I\omega)|C_I|^2 + \frac{1}{4H} \rho(\beta_c + 2p_I\omega)|T_I|^2. \quad \text{(A8)}$$

The energy flux away from the trench is

$$-\frac{1}{4} \rho g' r^2(\beta_c + 2k_R\omega)|C_I|^2$$
$$-\frac{1}{4H} \rho(\beta_c + 2p_R\omega)|T_R|^2, \quad \text{(A9)}$$

since by (3.10) $|C_R| = |C_I|$. The baroclinic contributions to the energy ($\propto |C_I|^2$) are equal in (A8) and (A9) because, by (3.5), $\beta_c + 2k_I\omega = -(\beta_c + 2k_R\omega)$, and baroclinic wave energy is conserved. Since $\psi/h = O(r^2 f)$, the barotropic contribution to the energy is smaller than the baroclinic part by a factor of H_1/H_2. Thus within the approximations of this model, the energy in the free barotropic mode in the deep ocean is negligible.

REFERENCES

Allen, J. S., 1975: Coastal trapped waves in a stratified ocean. *J. Phys. Oceanogr.*, **5,** 300–325.

Brink, K. H., 1982: A comparison of long coastal trapped wave theory with observations off Peru. *J. Phys. Oceanogr.*, **12,** 897–913.

——, 1983: Some effects of stratification on long trench waves. *J. Phys. Oceanogr.*, **13,** 496–500.

Busalacchi, A. J., and J. J. O'Brien, 1981: Interannual variability of the Equatorial Pacific in the 1960's. *J. Geophys. Res.*, **86,** 10 901–10 907.

Emery, W. J., W. G. Lee and L. Magaard, 1984: Geographical and seasonal distributions of Brunt-Väisälä frequency and Rossby radii in the North Pacific and North Atlantic. *J. Phys. Oceanogr.*, **14,** 294–317.

Gratton, Y., 1983: Low-frequency vorticity waves over strong topography. Ph.D. thesis, University of British Columbia, 143 pp.

Kang, Y. Q., and L. Magaard, 1980: Annual baroclinic Rossby waves in the central north Pacific. *J. Phys. Oceanogr.*, **10,** 1159–1167.

LeBlond, P. H., and L. A. Mysak, 1978: *Waves in the Ocean.* Elsevier, 602 pp.

Magaard, L., 1983: On the potential energy of baroclinic Rossby waves in the North Pacific. *J. Phys. Oceanogr.*, **13,** 38–42.

Mysak, L. A., 1983: Generation of annual Rossby waves in the North Pacific. *J. Phys. Oceanogr.*, **13,** 1908–1923.

——, 1984: Topographic waves in lakes. *Hydrodynamics of Lakes,* K. Hutter, Ed., Springer-Verlag, 81–128.

——, and A. J. Willmott, 1981: Forced trench waves. *J. Phys. Oceanogr.*, **11,** 1481–1502.

——, and L. Magaard, 1983: Rossby wave driven Eulerian mean flows along nonzonal barriers, with application to the Hawaiian Ridge. *J. Phys. Oceanogr.*, **13,** 1716–1725.

——, P. H. LeBlond and W. J. Emergy, 1979: Trench waves. *J. Phys. Oceanogr.*, **9,** 1001–1013.

Suarez, A. A., 1971: The propagation and generation of topographic oscillations in the ocean. Ph.D. thesis, M.I.T., 196 pp.

White, W. B., and J. F. T. Saur, 1981: A source of annual baroclinic waves in the eastern subtropical North Pacific. *J. Phys. Oceanogr.*, **11,** 1452–1462.

Willmott, A. J., and A. A. Bird, 1983: Freely propagating trench waves on a beta-plane. *J. Phys. Oceanogr.*, **13,** 1659–1668.